Materials Chemistry and Physics 225 (2019) 399–405

Contents lists available at ScienceDirect

Materials Chemistry and Physics

journal homepage: www.elsevier.com/locate/matchemphys

Partially sulfonated styrene-(ethylene-butylene)-styrene copolymers: Nanostructures, bio and electro-active properties

Ilghar Orujalipoor[a,h], Kinyas Polat[b], Yen-Chih Huang[d,e], Semra İde[f,*], Murat Şen[c], U-Ser Jeng[d,e], Gözde Koşarsoy Ağçeli[g], Nilüfer Cihangir[g]

[a] Institute of Science, Dept. of Nanotechnology and Nanomedicine, Hacettepe University., Beytepe, 06800, Ankara, Turkey
[b] Dept. of Chemistry, Dokuz Eylul University, Tınaztepe, 35390, Izmir, Turkey
[c] Dept. of Chemistry, Hacettepe University, Beytepe, 06800, Ankara, Turkey
[d] National Synchrotron Radiation Research Center, Hsinchu 30076, Taiwan
[e] Dept. of Chemical Eng., National Tsing Hua University, Hsinchu 30013, Taiwan
[f] Dept. of Physics Eng., Hacettepe University, Beytepe, 06800, Ankara, Turkey
[g] Dept. of Biology, Hacettepe University, Beytepe, 06800, Ankara, Turkey
[h] Alptek Engineering and Technological Systems A. S., Umraniye, 34774, Istanbul, Turkey

HIGHLIGHTS

- Nano structured electro- and bio-active SSEBS copolymers have been obtained by sulfonation.
- Nano and micro scale characterizations showed structural changes by the effect of sulfonation.
- Effective radius of nanoglobules increase up to 4 min sulfonation time and then decrease.
- 4 min sulfonation causes optimum nanoglobular size and new microsized clustering.
- The SSEB-films exhibited stronger antibacterial than antifungal activity.

GRAPHICAL ABSTRACT

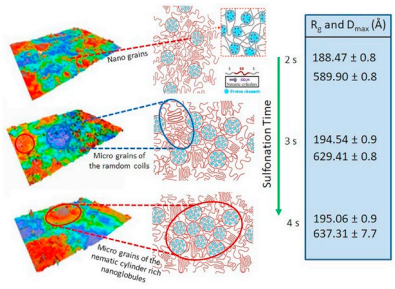

ARTICLE INFO

Keywords:
Morphology
SAXS
Antimicrobial activity
SEBS
Copolymer

ABSTRACT

Conductive polymers take much interest because of their electroactive definition as new generation smart biomaterials beside of their potential usage in proton exchange membrane fuel cells. Partially sulfonated styrene-(ethylene-butylene)-styrene (sSEBS) triblock copolymer based films (coded SEBS68 with the content of 68% SEBS, 5% PP, 26,5% Wax and 0,5% stabilizer) have been focused in the present study. Chemical manipulations have been done during the synthesis of the films for formation of nano-scale cylindrical like globular and lamellar like nematic aggregations. Association of the nano aggregations and nano-domains in the films were investigated by using small- and wide-angle X-ray scattering methods. Microscale surface morphologies and features were also examined by a compact non-contact 3D surface profiler system. The results show that the changes in the nanostructures and the surface morphologies are dependent on sulfonation time. With sulfonation time of 4 min, the system could reach optimum physico-chemical properties, including the optimized size of phase segregation tunnels. It was also found that the modified polymer morphologies with nanostructural features are effective on antimicrobial activities against the different test microorganisms studied.

* Corresponding author.
E-mail address: side@hacettepe.edu.tr (S. İde).

https://doi.org/10.1016/j.matchemphys.2018.12.029
Received 24 May 2018; Received in revised form 19 November 2018; Accepted 12 December 2018
Available online 13 December 2018
0254-0584/ © 2018 Elsevier B.V. All rights reserved.

1. Introduction

After the Nobel Prize for chemistry to Heeger and Shirakawa for discovery about the conducting properties of polyacetylene, nine different groups of conducting materials have been introduced up to now such as polythiophenes, polypyrroles, polyanilines, polyfurans, polycarbazoles. These polymers have −CH groups which can be substituted with other chemical groups to change their electronic or ionic conductivity, optical properties, mechanical properties, stored charges, stored ions, sensing properties [1–5]. Among those groups self-doped conducting polymers where the substituent group is an ionic group bonded covalently to a monomeric unit and the other ion-exchanged with the electrolyte opens up the door for soluble conducting polymers [6–8].

Polystyrene-block-poly-(ethylene-ran-butylene)-block-polystyrene (SEBS) triblock copolymer is an interesting abundant material for industrial and technological science because of its eligibility towards ion conducting and electroactive properties, different nanoscale structural designs, physico-chemical properties, bioactivities and its thermoplastic-elastomeric duality [9,10].

SEBS shows elastomeric property like chemically crosslinked polymers [11].

However, SEBS does not contain any chemical crosslink. Instead, it has physical crosslinks due to the aggregation of styrene domains. When heat is applied, these physical crosslinks disappear converting the structure to a thermoplastic material that can be processed by an extruder. But when cooled to room temperature, those domains are recreated forming an elastomer structure. Despite the advantage of this duality, it is not easy to make thinner SEBS films for variety of useful applications such as membrane materials, antimicrobial films because the films obtained after heat treatment do not maintain their forms and immediately shrink and deform [12,13].

Therefore, in this study, SEBS thin films were prepared as composite by using polypropylene (PP) and wax. Due to the aliphatic structure of both PP and wax, ethylene and butylene domains in the SEBS are reinforced enabling to make thinner films of SEBS up to 125 μm or much smaller. Nano structural design by chemical means can introduce some other properties to the SEBS structure. One of the chemical means is the sulfonation of benzene groups on the backbone by chlorosulfonic acid solution for different durations. Depending on the sulfonation time, several nanostructures are built such as nano-cylinders, nano-tunnels or lamellar domains due to the phase segregation between hydrophobic ethylene-butylene domains and hydrophilic benzene sulfonic acid groups [14–21]. In this respect, it is highly important to create a well ordered and uniform nanostructure. A balance has to be achieved between the uniformity and density of the nano-structures in the polymer matrix.

In this work, nano-structures and microscale surface morphologies of the sulfonated SEBS68 (which consist of 68% SEBS, 5% PP, 26,5% Wax and 0,5% stabilizer) films were examined. The main question was “How are the self-assembled nano tunnels and the surface morphologies structurally changing with the sulfonation time?“. First of all, surface profiles were investigated by a Sensofar 3D non-contact profilometer system (multi-national company) then, small- and wide-angle X-ray scattering (SAXS and WAXS) analyses were applied to examine structural information about uniformities, aggregate size, shape, distance distributions of aggregates/aggregate stacks and nano ordering of the studied polymer composite films.

The basic nanoscale structural features of the focused composites were examined in previous work [22]. The development of polymers with antimicrobial properties is an important area of research focused on different fields of applications, like hospital environment (surfaces/furniture), surgery equipments, water purification systems, food packaging and storage, antifouling paints, etc. [23]. The surface modifications and the synthesis of new designed polymer-based nanocomposites are also important for attractive strategies to achieve more permanent antimicrobial effects. Some woven textiles such as cotton, wool, nylon and polyester may be covered with this studied type nanocomposites to develop antimicrobial properties.

Along with this work, a detailed nanostructural analysis has been carried out on sSEBS and for the first time antimicrobial properties have been investigated to determine their potential usage as cost-effective antimicrobial materials.

2. Experimental

2.1. Materials and chemicals

Styrene-(ethylene-buthylene)-styrene (SEBS) consisting of 31.5% (w/w) styrene and 68.5% (w/w) ethylene-butylene obtained from Kraton Performance Polymers Inc., Texas, USA with a molecular weight of 95000 g/mol. Wax (Finewax EI) was purchased from Fine Organics, Mumbai, India. Polypropylene PP (MH 418) was purchased from Petkim Petrokimya Holding A.Ş, Izmir, Turkey with melt flow index of 4–6 g/10 min. Stabilizer (Irganox) granules, made up of pentaerythritol tetrakis(3-(3,5-di-tert-butyl-4- hydroxyphenyl)propionate) with a melting point of 85 °C, was purchased from BASF S.A. Chlorosulfonic acid and 1,2-dichloro-ethane were purchased from Sigma-Aldrich Co. LLC. and Merck & Co., respectively.

2.2. Preparation of the films

SEBS were extruded by using a Reomex OS model (Thermo–Haake) laboratory-type twin screw extruder at 80 g/min feed rate. The temperature of the extruder was kept at 180 °C at the entrance, 210 °C in the barrel and 180 °C at the extruder tip. Thinner films were obtained from a rolling-stretching unit that was positioned at 30 cm across. 125 μm thickness was further done via a hot-press. Films were sulfonated by immersing in a chlorosulfonic acid solution in 1,2-dichloroethane for different times and neutralized by methanol–water mixture, then washed with deionized water [24]. Degree of sulfonation is linear up to the 5 min and then begin to decrease due to the chain scission effect of chlorosulfonic acid overexposure. The variation of degree of sulfonation with time is given in Table 1.

2.3. Characterization methods

Sensofar 3D non-contact profilometer DEMO measurements were carried out for the SEBS films of different durations of sulfonation by using a surface profiler system. Surface indentation and protrusion range of ΔZ may be measured along the verticle (Z) axis and the maximum horizontal (X) range is also informative for the surface properties and more stable structural character of the surfaces. For the ideal samples ΔZ and maximum X values should be small and big respectively.

Synchrotron-based small- and wide-angle X-ray scattering (SAXS and WAXS) measurements were simultaneously conducted to examine the self-organization of nanoaggregates and their ordered arrays in the studied membrane films. The structural size and orientation information of both the donor and acceptor domains in the sulfonated films provide a better understanding of the physicochemical mechanism of

Table 1
The variation of degree of sulfonation with time.

Time(min)	Degree of Sulfonation (%)
2	40.8
3	64.5
4	65.2
5	97.5
45	87.3
60	76.4

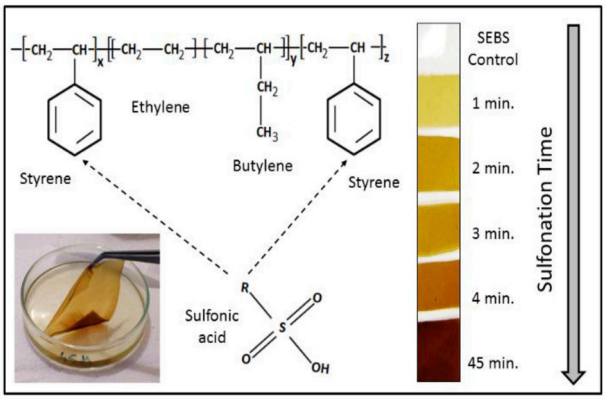

Fig. 1. Molecular Scheme of SEBS and the illustration of the sSEBS samples with the sulfonation time.

Table 2
Elemental composition of the membranes determined by EDS.

Sulfonation time (min)	Carbon %	Sulfur %
1	89.2	10.8
2	88.4	11.5
3	88.4	11.6
4	84.4	15.6
45	27.0	73.0

carrier transport. Small and wide angle X-ray scattering (SWAXS) experiments were performed at the BL23A SWAXS end-station of the National Synchrotron Radiation Research Center, Hsinchu, Taiwan [25].

2.4. Characterization antimicrobial activity

The antimicrobial activity of the sulfonated SEBS composites was evaluated against Gram positive bacteria *Staphylococcus aureus* (ATCC 29213), Gram negative bacteria *Escherichia coli* (ATCC 35218), yeast *Candida albicans* and mold *Aspergillus niger*. 0,1 ml *Staphylococcus aureus* (ATCC 29213) and *Escherichia coli* (ATCC 35218) were adjusted to 0.5 McFarland turbidity standard inoculated of Mueller-Hinton Agar culture medium, 0,1 ml *Candida albicans* culture was adjusted to 0.5 McFarland turbidity standard inoculated of Potato Dextrose Agar (PDA) and 0,1 ml *Aspergillus niger* culture was adjusted spore suspension (1×10^6/ml) inoculated of Potato Dextrose Agar (PDA) with sterile swab. Circular pieces of composites (5 mm in diameter) were used for antimicrobial tests. SEBS composites which were exposed to UV were placed onto an inoculated surface as an antibiotic disk. The bacteria plates were incubated at 37 °C and fungi plates were incubated at 30 °C for 24 h, and the inhibition zone diameters were measured.

3. Results and discussion

Structure of pure SEBS and position of sulfonic acid groups on the benzene ring after sulfonation are given in Fig. 1. The color change related to the sulfonation time is also introduced the figure. Amount of the sulfonic acid groups in the structure has been determined by weight increase due to the SO_3 groups and calculated by using the equation (1).

$$SD\ \% = \left[\frac{\left[\frac{(M_{as} - M_{bs})}{M_{SO_3}} \right]}{M_{bs} \left(\frac{Styrene\ block\ \%}{Styrene\ block\ molecular\ weight} \right)} \right] 100 \quad (1)$$

where SD stands for sulfonation degree, M_{bs} is membrane weight before sulfonation, M_{as} is membrane weight after sulfonation and M_{SO3} is the molecular weight of SO_3 group. Elemental compositions of the membranes were also identified by SEM-EDS analyses. Elemental compositions with respect to carbon and sulphur content were collected in the

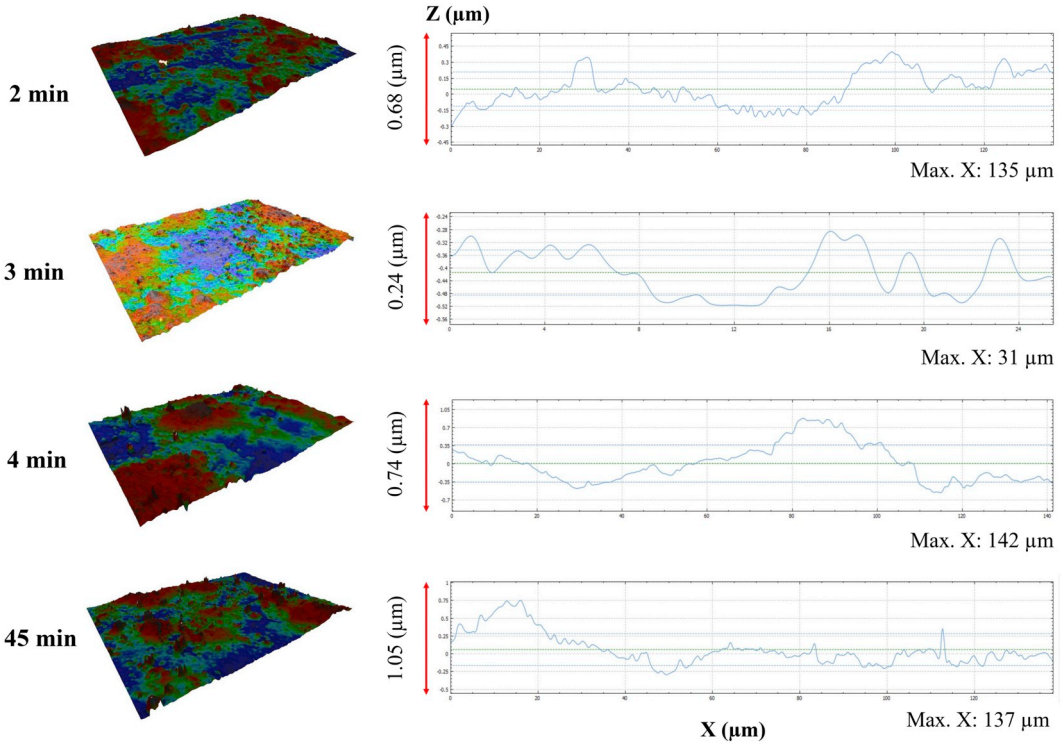

Fig. 2. 3D surface morphologies of the sSEBS films of different sulfonation times as indicated including the maximum ranges along surface parallel x axis and the depth measures for the wavy surface character.

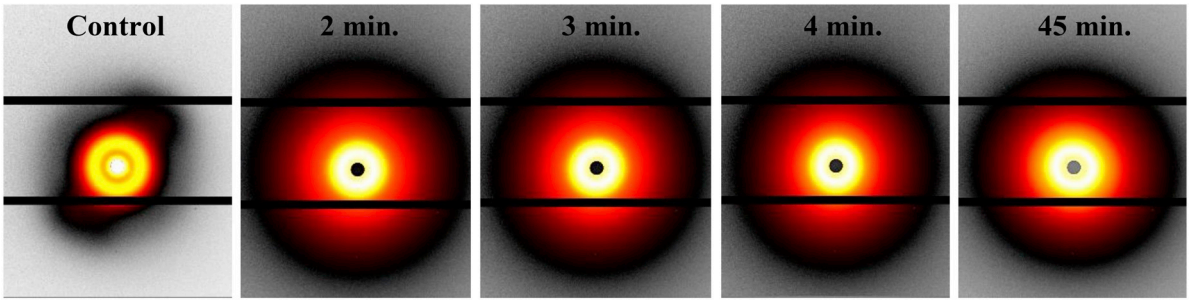

Fig. 3. 2D SAXS patterns of the studied samples of different sulfonation time as indicated.

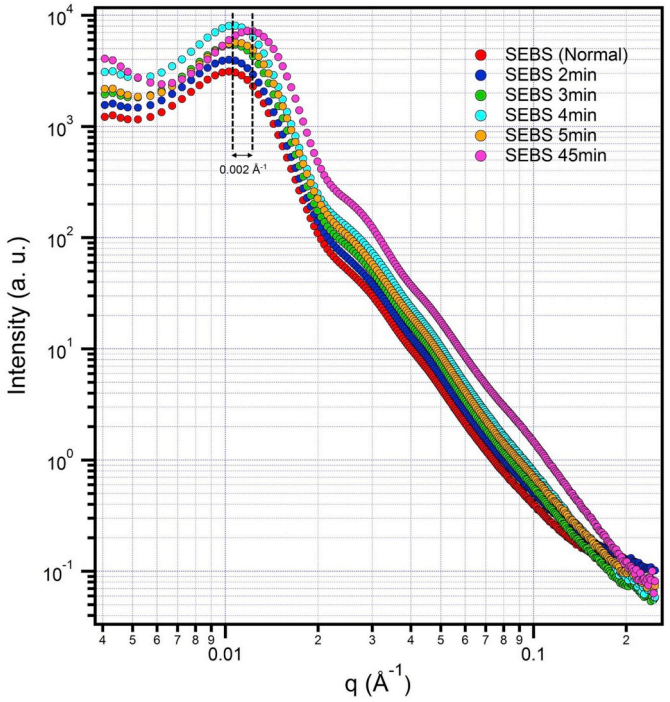

Fig. 4. SAXS profiles of the studied SEBS and sSEBS composites.

Table 3
The radius of gyration value (R_g), maximum size of the globular phase segregation channels and the obtained χ^2 values after the widely used refinement process [22].

Samples	R_g (Å)	D:Max. Extent (Å)	Chi Square Value
SEBS-Normal	194.8 ± 0.9	624.97 ± 0.7	2.2
SEBS-2min	188.47 ± 0.8	589.90 ± 0.8	6.2
SEBS-3min	194.54 ± 0.9	629.41 ± 0.8	4.2
SEBS-4min	195.06 ± 0.9	637.31 ± 7.7	4.7
SEBS-5min	192.74 ± 2.3	641.84 ± 3.5	3.3
SEBS-45min	185.12 ± 2.8	616.56 ± 3.7	1.5

Table 2.

Topographic visualizations and surface profile along z axis toward the depth of the membrane thickness were obtained as seen in Fig. 2.

Surface indentation and protrusion range (0.74 μm, Fig. 2) is less and the maximum X value is the biggest (142 μm) for the 4 min sulphonated sample respect to the other sSEBS 45 min sample.

The recorded 2D SAXS data for the SEBS control and sSEBS films were shown in Fig. 3.

The corresponding SAXS profiles of $I(q)$ vs. q circularly averaged from the corresponding isotropic 2D patterns data was given in Fig. 4. Here, $q = 4\pi\lambda^{-1}\sin\theta$ is the wave vector transfer defined by the X-ray wavelength λ and the scattering angle 2θ. There was no observable peaks in the WAXS profiles with range of 2.8–8.3 Å. So it may be said that, the sulfonation does not cause structural change in the molecular scaled crystalline structure of the samples.

At the starting point of the detailed scattering analysis, nanostructural models were constructed by using convenient form factors related to the expectations about the nano aggregations [26,27]. The previously published cylindrical form factor (for the control group) was also used for sulfonated samples by using IGOR pro [28].

Nanostructural characteristics are effectively changing as seen in the SAXS profiles (Fig. 4). The sulpfonated SEBS 4 min and SEBS 45 min samples have sharper peaks respect to the other samples at q = 0.013 and 0.027, $Å^{-1}$. The sharp peaks imply ordered inner arrangements and the difference in the peak positions at q axis is caused by the different predominant structural length scale in the volume of the studied films [29].

The biggest sulfonation time (of 45 min) results smaller nematic packing feature with cylindrical like globular (nematic) tunnels but their low ordered arrangements respect to that of SEBS 4 min, as evidenced from the rightward deviation in the intense SAXS peak of SEBS 45 min sample respect to that of SEBS 4 min. Rg and maximum extend values (Table 3) of the SEBS 45 min is smaller than those of SEBS 4 min and this suggests larger nematic domains with high ordered nematic phase segregation tunnels and their bigger interplanar like distance in the structure of SEBS 4 min sample respect to 45 min. The mentioned nematic ordering peak positions of SEBS 45 min were determined at q = 0.013 and 0.027 $Å^{-1}$. Interplanar distance of d (d = 2π/q) of the slightly distorted nematic (lamellar like) arrayed tunnels decreases with the higher sulfonation time by 8.8 nm, decreased from 57.1 nm (q = 0.013 $Å^{-1}$) to 48.3 nm (q = 0.027 $Å^{-1}$) for 4 and 45 min sulfonated samples. Fig. 5 shows the fitted higher-q SAXS curves and Pair Distance Distributions of the nano tubular aggregations for 45 min and 4 min sulfonated samples, to avoid the interference effect in form factor determination. It may stem from the intercalating effect of chain parts containing styrene sulfonic acid due to the chain scission at high sulfonation times.

Sulfonation effects marginally the size of the phase segregation tunnels but it certainly effect the mean distribution of the tunnels and ordered domains sizes with the increasing sulfonation time, as seen in Table 3.

The radius of gyration values of the phase segregation tunnels (nanocylinders) were obtained in the range of 185 ± 3–195 ± 1 Å for all samples. 4 min sulfonation is causing the biggest (R_g = 195.06 ± 0.9 Å) nano globules in the structure. The biggest effect of the sulfonations was obtained for the sulfonated SEBS 4 and 45 min samples.

It was known that SEBS nano aggregations have a synergistic effect on the balanced mechanical performance of the polymer composites [30]. The size range of the phase segregation tunnels is also important to cause the potential antimicrobial properties against different test micro-organisms. It was also known that the polymeric materials with antimicrobial activities have usually the size range of 60–200 nm [23]. According to the unchanging WAXS profiles, the aggregate styrene

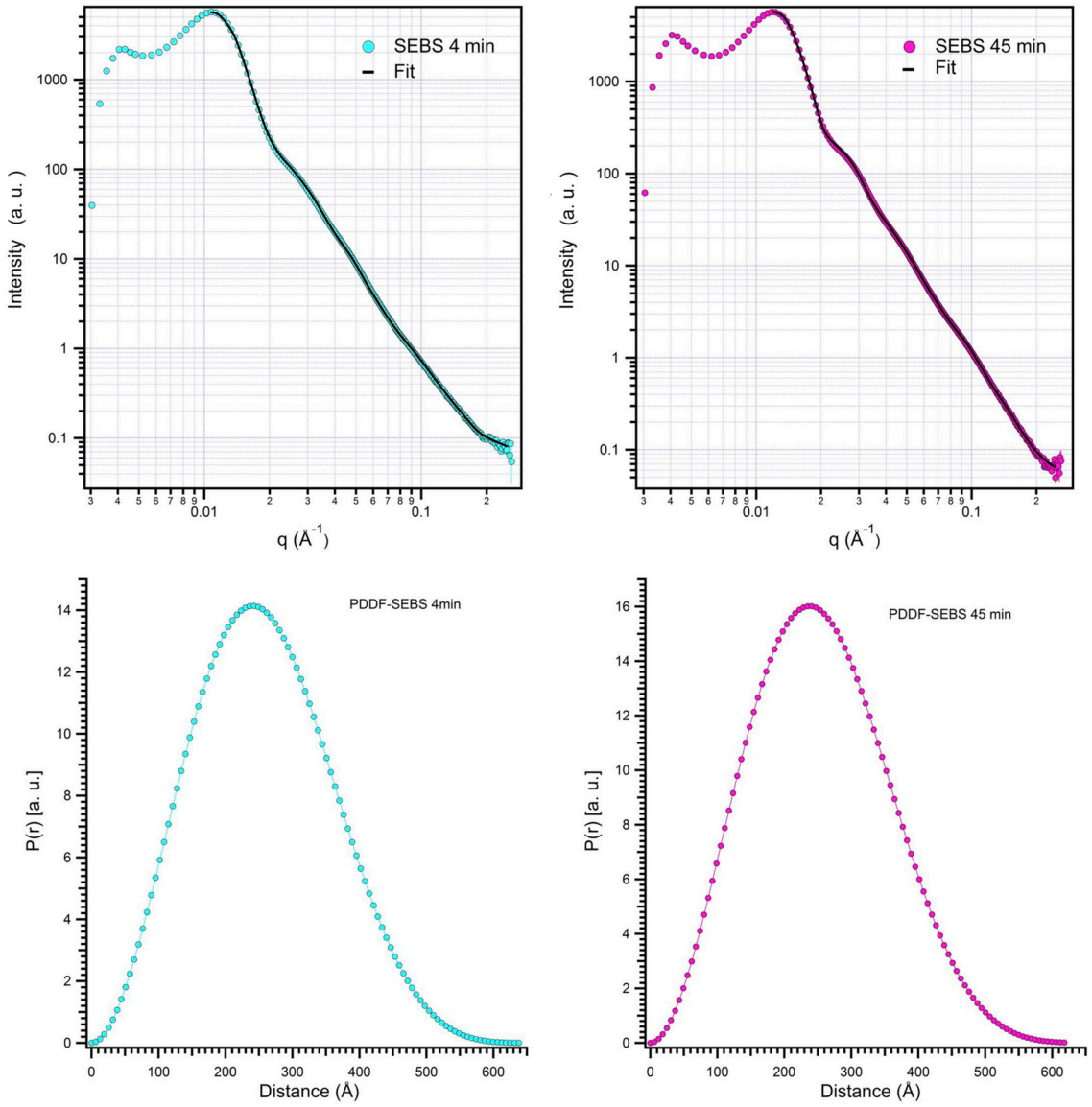

Fig. 5. The fitting illustrations for SEBS 4 min and SEBS 45 min samples (upper row); the corresponding pair distance distributions P(*r*) of the cylindrical-like (globular) phase segregation tunnels under the effect of 4 min and 45 min sulfonation times.

Table 4
Measured characteristics of the 4 min sulfonated sample.

Carbon (left) and Sulfur (right) profiles of the sample defined by EDX spectra (S/C = 18%)

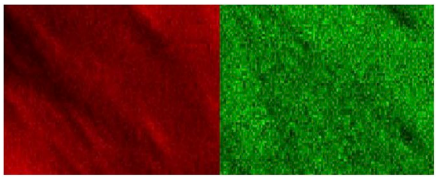

SEM view of the sample (SEMSystem:JEOL JSM5600LV)

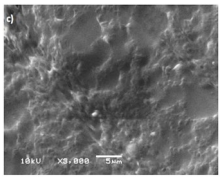

Electrical resistance of the membrane: 65.5 Ω cm at T = 25 °C
Conductivity: 191.0 mScm^{-1} for 100% moisture at T = 25 °C

Total Membrane Thickness: 125 ± 5 μm
Energy of surface tension: 50 mJm^{-2}

domain structures of the SEBS films are stable under sulfonation. So, it may be said that, the nano globular self-assembled aggregations are the major factor to define the properties of the membrane films in the following application shown below.

The surface texture of the 4min. sulfonated sample was also easily determined with respect to the others in bigger x-range (along to the parallel direction to the surface) of 142 μm. The optimum thickness including wavy surface was measured for this sample as 0.74 μm. The surface morphology of SEBS 45 min sample has sharp peaks and big vertical deviation (1.05 μm)according to the surface. This structural property is also indicating preferable sample is SEBS 4 min for the technological applications. The other important features with the effective 4 min sulfonated sample were also determined, with the corresponding physico-chemical properties summarized briefly in Table 4

Table 5
Inhibition zones (mm) of the sulfonated samples and two representative zones. As known that the measured bigger zones than 5 mm* are evidence of more bioactive properties of the membranes.

Microorganisms	SEBS-1 min	SEBS-2 min	SEBS-3 min	SEBS-4 min	SEBS-5 min	SEBS-45 min
E.coli	5 mm*	10 mm	5 mm*	8 mm	5 mm*	9 mm
S.aureus	5 mm*	9 mm	8 mm	5 mm*	15 mm	11 mm
Candida albicans	–	–	–	–	–	–
Aspergillus niger	5 mm*	5 mm*	5 mm*	5 mm*	5 mm*	5 mm*

[24].

Surface tension energy is lower for 45 min sulfonated sample (20 mJm^{-2}) respect to 4 min sulfonated sample (50 mJm^{-2}). More parallel arrangements and tighter packing (shorter inter tubular distances) of the nanotubular structures in longer sulfonation times may be responsible for this lower tension.

In Table 5, the growth inhibited areas with the sulfonated SEBS films are shown for the antimicrobial effects. The results show that 1 min sulphonated sample did not effect on *E.coli* and *S.aureus* while 2 min and 45 min sulphonated samples were effective on suppressing of *E.coli* and *S.aureus*. 3 min and 5 min sulphonated samples were effective only their diameter (5 mm) on *E.coli* but they were effective on *S.aureus* (8 mm and 15 mm). 4 min sulphonated sample was effective only their diameter (5 mm) on *S.aureus* but it was effective on *E.coli* (8 mm). Moreover, SEBS films had marginal effect on *Aspergillus niger* viability. The zone of inhibition was measured only films diameter. However, the films did not inhibit the growth of *Candida albicans*. Moreover, SEBS films demonstrated a stronger influence on bacteria than fungi. Similar to bacteria, the cytoplasmic membrane of a fungus is surrounded by a cell wall structure. Unlike bacteria, the fungal cell walls are lamellar with each layer consisting of fibrils crisscrossing one another in various direction. The principal constituents of the fungal cell wall are various types of polysaccharides with minor amounts of lipid and protein. Chitin has been reported as the common polysaccharide component present in all fungal cell walls. Fungi are known to survive in severely stressful conditions where bacteria cannot [31,32].

4. Conclusion

In this work, we have mainly demonstrated the effect of sulfonation time on the focused SEBS film which has potential applications in antimicrobial activity. It was obtained that, sulfonation is effective on the distributions of nanoglobular cylindrical like globular (nematic) tunnels and their sizes. The nano scaled ordering increases with the bigger sulfonation time as obtained by the SAXS profiles (Fig. 4) and the 4 min and 45 min sulfonation cause stable and high ordered inner arrangement in nano scale respect to the other durations. The transparency of the sulfonated SEBS 4 min sample may be preferable for the technological applications. The resultant information including energy of surface tension, total membrane thickness and the depth of surface indentations may be accepted for more efficient, reproducible and traceable manufacturing of sSEBS films.

The microbiological assay showed a reduction over in *E.coli* with 2, 4 and 45 min sulfonated samples and in *S.* aureus with 2, 3, 5, 45 min sulfonated samples. The maximum inhibition zone was seen SEBS-5 min. for *S.aureus* (15 mm).

This work briefly shows that, 4 min sSEBS films are potentially useful in nano technological developments as nano-structured membranes with electroactive and bioactive properties.

Acknowledgement

We would like to thank Alberto Aguerri and Sensofar company for providing the chance of S-lynx non-contact compact 3D optical profiler usage.

References

[1] C. Chiang, C. Fincher, Y. Park, A. Heeger, H. Shirakawa, E. Louis, S. Gau, A. MacDiarmid, Electrical conductivity in doped polyacetylene, Phys. Rev. Lett. 39 (1977) 1098–1101.
[2] H. Shirakawa, E. Louis, A. MacDiarmid, C. Chiang, A. Heeger, Synthesis of electrically conducting organic polymers: halogen derivatives of polyacetylene, (CH)x, J. Chem. Soc., Chem. Commun. (1977) 578–580.
[3] T.F. Otero, Biomimetic conducting polymers: synthesis, materials, properties, functions, and devices, Polym. Rev. 53 (2013) 311–351.
[4] J. Roncali, Synthetic principles for bandgap control in linear π-conjugated systems, Chem. Rev. 97 (1997) 173–205.
[5] M. Jaymand, Recent progress in chemical modification of polyaniline, Prog. Polym. Sci. 38 (2013 1287–1306).
[6] A. Patil, Y. Ikenoue, F. Wudl, A. Heeger, Water soluble conducting polymers, J. Am. Chem. Soc. 109 (1987) 1858–1859.
[7] L. Li, K.E. Counts, S. Kurosawa, A.S. Teja, D.M. Collard, Tuning the electronic structure and solubility of conjugated polymers with perfluoroalkyl substituents: poly(3-perfluorooctylthiophene), the first supercritical CO2-soluble conjugated, PolymerAdv. Mater. 16 (2004) 180–183.
[8] E. Yildiz, P. Camurlu, C. Tanyeli, I. Akhmedov, L. Toppare, A soluble conducting polymer of 4-(2,5-di(thiophen-2-yl)-1H-pyrrol-1-yl)benzenamine and its multichromic copolymer with EDOT, J. Electroanal. Chem. 612 (2008) 247–256.
[9] T.J. Rivers, T.W. Hudson, C.E. Schmidt, Synthesis of a novel, biodegradable electrically conducting polymer for biomedical applications, Adv. Funct. Mater. 12 (2002) 33–37.
[10] R. Balint, N.J. Cassidy, S.H. Cartmell, Conductive polymers: towards a smart biomaterial for tissue engineering, Acta Biomater. 10 (2014) 2341–2353, https://doi.org/10.1016/j.actbio.2014.02.015.
[11] J.M. Serpico, S.G. Ehrenberg, J.J. Fontanella, X. Jiao, D. Perahia, K.A. McGrady, E.H. Sanders, G.E. Kellogg, G.E. Wnek, Transport and structural studies of sulfonated styrene-ethylene copolymer membranes, Macromolecules 35 (2002) 5916–5921, https://doi.org/10.1021/ma020251n.
[12] J. Kim, B. Kim, B. Jung, Proton conductivities and methanol permeabilities of membranes made from partially sulfonated polystyrene-block-poly(ethylene-ran-butylene)-block-polystyrene copolymers, J. Membr. Sci. 207 (2002) 129–137, https://doi.org/10.1016/S0376-7388(02)00138-2.
[13] B. Kim, J. Kim, B. Jung, Morphology and transport properties of protons and methanol through partially sulfonated block copolymers, J. Membr. Sci. 250 (2005) 175–182, https://doi.org/10.1016/j.memsci.2004.10.025.
[14] P. Sengupta, Morphology of Olefinic Thermoplastic Elastomer Blends, University of Twente, 2004.
[15] H. Veenstra, B.J.J. Van Lent, J. Van Dam, A. Posthuma De Boer, Co-continuous morphologies in polymer blends with SEBS block copolymers, Polymer (Guildf) 40 (1999) 6661–6672, https://doi.org/10.1016/S0032-3861(98)00875-1.
[16] H. Mae, M. Omiya, K. Kishimoto, Toughening mechanism of PP with bimodal distributed SEBS particle size, Soc. Exp. Mech. - 11th Int. Congr. Exhib. Exp. Appl. Mech, vol. 2008, 2008, pp. 233–239.
[17] H.Y. Hwang, H.C. Koh, J.W. Rhim, S.Y. Nam, Preparation of sulfonated SEBS block copolymer membranes and their permeation properties, Desalination 233 (2008) 173–182, https://doi.org/10.1016/j.desal.2007.09.040.
[18] T.B. Ohlsson B, Hassender H, blends and thermoplastic interpenetrating polymer networks of polypropylene and polystyrene-block- Poly (EthyIene-stat-Butylene)-block-Polystyrene triblock copolymer. 1: morphology and structure-related properties, Polym. Eng. Sci. 36 (1996) 501–510, https://doi.org/10.1002/pen.10436.
[19] A. Mokrini, M.A. Huneault, Z. Shi, Z. Xie, S. Holdcroft, Non-fluorinated proton-exchange membranes based on melt extruded SEBS/HDPE blends, J. Membr. Sci.

325 (2008) 749–757, https://doi.org/10.1016/j.memsci.2008.08.051.
[20] P. Sengupta, J.W.M. Noordermeer, A comparative study of different techniques for microstructural characterization of oil extended thermoplastic elastomer blends, Polymer (Guildf) 46 (2005) 12298–12305, https://doi.org/10.1016/j.polymer.2005.10.075.
[21] A. Mokrini, M.A. Huneault, Proton exchange membranes based on PVDF/SEBS blends, J. Power Sources 154 (2006) 51–58, https://doi.org/10.1016/j.jpowsour.2005.04.021.
[22] K. Polat, I. Orujalipoor, S. Ide, M. Şen, Nano and microstructures of SEBS/PP/wax blend membranes, SAXS and WAXS analyses, J. Polym. Eng. 35 (2015) 151–157, https://doi.org/10.1515/polyeng-2014-0093.
[23] A. Muñoz-Bonilla, M. Fernández-Garc'ia, Polymeric materials with antimicrobial activity, Prog. Polym. Sci. 37 (2012) 281–339, https://doi.org/10.1016/j.progpolymsci.2011.08.005.
[24] K. Polat, Development of Styrene-(ethylene-buthylene)-styrene (SEBS) Based Composite Polyelectrolyte Membrane for Fuel Cell Applications, HACETTEPE, 2013.
[25] U.S. Jeng, C.H. Su, C.J. Su, K.F. Liao, W.T. Chuang, Y.H. Lai, J.W. Chang, Y.J. Chen, Y.S. Huang, M.T. Lee, K.L. Yu, J.M. Lin, D.G. Liu, C.F. Chang, C.Y. Liu, C.H. Chang, K.S. Liang, A small/wide-angle X-ray scattering instrument for structural characterization of air-liquid interfaces, thin films and bulk specimens, J. Appl. Crystallogr. 43 (2010) 110–121, https://doi.org/10.1107/S0021889809043271.
[26] G. Porod, O. Glatter, O. Kratky, In Small Angle X-ray Scattering, Acad. Press., 1982, p. 515.
[27] L.A. Feigin, D.I. Svergun, Structure Analysis by Small-angle X-Ray and Neutron Scattering, (1987), https://doi.org/10.1007/978-1-4757-6624-0.
[28] S.R. Kline, Reduction and analysis of SANS and USANS data using IGOR Pro, J. Appl. Crystallogr. 39 (2006) 895–900, https://doi.org/10.1107/S0021889806035059.
[29] L. Song, W. Wang, S. Pröller, D.M. Gonzalez,ˊJ. Schlipf, C.J. Schaffer, K. Peters, E.M. Herzig, S. Bernstorff, T. Bein, D. Fattakhova-Rohlfing P, In situ study of degradation in P3HT – TitaniaBased solid-state dye-sensitized solar cells, müller-buschbaum, ACS Energy Lett 2 (2017) 991–997.
[30] F.H. Su, H.X. Huang, Mechanical and rheological properties of PP/SEBS/OMMT ternary composites, J. Appl. Polym. Sci. 112 (2009) 3016–3023, https://doi.org/10.1002/app.29875.
[31] J.M. Arnoson, The cell wall, in: G.C. Ainsworth, A.S. Sussman (Eds.), The Fungi, vol. 1, Academic Press, New York, NY, 1965, pp. 49–76.
[32] S. Bartnicki-Garcia, J.M. Ashworth, J.E. Smith (Eds.), "Fundamental Aspects of Hyphal Morphogenisis," Microbial Differentiation, Cambridge University Press, London, UK, 1973, pp. 245–267.